

1-1-2015

Effect of Methoxylated Sites in Sn-Beta Zeolite on Glucose Transformations

Caterina Tran

Follow this and additional works at: <https://scholarsjunction.msstate.edu/td>

Recommended Citation

Tran, Caterina, "Effect of Methoxylated Sites in Sn-Beta Zeolite on Glucose Transformations" (2015).
Theses and Dissertations. 1669.
<https://scholarsjunction.msstate.edu/td/1669>

This Graduate Thesis - Open Access is brought to you for free and open access by the Theses and Dissertations at Scholars Junction. It has been accepted for inclusion in Theses and Dissertations by an authorized administrator of Scholars Junction. For more information, please contact scholcomm@msstate.libanswers.com.

Effect of methoxylated sites in Sn-Beta zeolite on glucose transformations

By

Caterina Tran

A Thesis
Submitted to the Faculty of
Mississippi State University
in Partial Fulfillment of the Requirements
for the Degree of Master of Science
in Chemical Engineering
in the Dave C. Swalm School of Chemical Engineering

Mississippi State, Mississippi

August 2015

Copyright by

Caterina Tran

2015

Effect of methoxylated sites in Sn-Beta zeolite on glucose transformations

By

Caterina Tran

Approved:

Neeraj Rai
(Major Professor)

Santanu Kundu
(Committee Member)

Hossein Toghiani
(Committee Member)

W. Todd French
(Graduate Coordinator)

Jason M. Keith
Interim Dean
Bagley College of Engineering

Name: Caterina Tran

Date of Degree: August 15, 2015

Institution: Mississippi State University

Major Field: Chemical Engineering

Major Professor: Dr. Neeraj Rai

Title of Study: Effect of methoxylated sites in Sn-Beta zeolite on glucose transformations

Pages of Study: 55

Candidate for Degree of Master of Science

Cellulose, a major constituent of biomass, is a promising source of sustainable energy. A key step in the conversion of cellulose to a platform chemical is glucose isomerization to fructose. Sn-Beta zeolite catalyzes this reaction with high yield. The effect of methanol as a reaction medium on glucose transformations catalyzed by Sn-Beta has not been quantified. Here, density functional calculations are employed to elaborate on the effect of methanol medium, specifically to determine how reaction pathways and energy barriers are affected by methoxylation of Sn or Si groups at the active sites in Sn-Beta. Calculations suggest that the presence of the neighboring silanol group is necessary for glucose isomerization. If the silanol group is altered by methoxylation glucose epimerization is promoted and will likely occur. These results provide additional understanding of the active site of Sn-Beta for glucose transformations and are insightful for novel catalyst design and development.

Key words: Sn-Beta zeolite, glucose isomerization, epimerization, methoxylation

DEDICATION

To Bó Mệ

ACKNOWLEDGEMENTS

First and foremost, I'd like to thank Dr. Rai. Thanks for your patience and guidance while I ventured my way through this world of research.

I would also like to thank Dr. H. and Dr. Kundu. Thank you for being a part of my committee and making me think more critically. Furthermore, I'd like to thank all of the Dave C. Swalm School of Chemical Engineering at Mississippi State University. Thanks for nurturing my mind and supporting my path for the past seven years.

I'd like to extend my appreciation to the National Energy Research Scientific Computing Center (NERSC). This research used resources of NERSC, a DOE Office of Science User Facility supported by the Office of Science of the U.S. Department of Energy under Contract No. DE-AC02-05CH11231.

Lastly, I want to thank my family and friends for their unending love, belief, and support. Without you, I would not have been able to complete this adventure.

Cecilia and Elizabeth, thanks for being the coolest kids I know.

Ian, thank you kindly for being my fairest.

TABLE OF CONTENTS

DEDICATION	ii
ACKNOWLEDGEMENTS	iii
LIST OF TABLES	vi
LIST OF FIGURES	vii
CHAPTER	
1. INTRODUCTION	1
2. COMPUTATIONAL DETAILS	8
2.1 First Hohenberg-Kohn Theorem	8
2.2 Second Hohenberg-Kohn Theorem	9
2.3 Kohn-Sham Method	11
2.4 Exchange Correlation Functional	12
2.5 Basis Set	12
2.6 Present Density Functional Theory Calculations	13
3. METHOXYLATION OF SITES IN SN-BETA ZEOLITE	17
3.1 Methoxylation of Sn Site	18
3.2 Methoxylation of Si Site	19
3.3 Summary	21
4. GLUCOSE ISOMERIZATION WITH METHOXYLATED SITES	22
4.1 Isomerization with Sn-Methoxylated Cluster	23
4.1.1 Monodentate Binding Mode	23
4.1.2 Bidentate Binding Mode	26
4.1.3 Summary	29
4.2 Isomerization with Si-Methoxylated Cluster	30

4.2.1	Monodentate Binding Mode	30
4.2.2	Bidentate Binding Mode	32
4.2.3	Summary	35
5.	GLUCOSE EPIMERIZATION WITH METHOXYLATED SITES	36
5.1	Epimerization with Sn-Methoxylated Site	37
5.1.1	Monodentate Binding Mode	37
5.1.2	Bidentate Binding Mode	39
5.1.3	Summary	41
5.2	Epimerization with Si-Methoxylated Site	41
5.2.1	Monodentate Binding Mode	41
5.2.2	Bidentate Binding Mode	43
5.2.3	Summary	45
6.	RESULTS AND DISCUSSION	46
7.	CONCLUSIONS	50
	REFERENCES	52

LIST OF TABLES

4.1	Activation Energies (kcal/mol) for Glucose Isomerization with Methoxylated Sn Site	29
5.1	Activation Energies (kcal/mol) for Glucose Epimerization with Methoxylated Sn Site	41
6.1	Activation Energies (kcal/mol) for Methoxylation at Sn and Si Site	46
6.2	Activation Energies (kcal/mol) for Glucose Transformations with Methoxylated Sn Site	47
6.3	Activation Energies (kcal/mol) for Glucose Transformations with Methoxylated Si Site	47

LIST OF FIGURES

1.1	Chemical structures of xylan and cellulose	2
1.2	Conversion of cellulose into a platform chemical	3
1.3	Molecular structure of beta zeolite framework	4
1.4	Framework Sn sites in Sn-Beta zeolite in closed and open forms	5
1.5	Scheme illustrating how reaction medium affects glucose transformation	6
2.1	Cluster model representations of Sn-Beta zeolite	14
2.2	Glucose binding modes	15
3.1	Methoxylation of Sn site in Sn-Beta zeolite	18
3.2	Methoxylation of Si site in Sn-Beta zeolite	20
4.1	Isomerization scheme	23
4.2	Initial proton transfer for glucose transformations in the monodentate mode with methoxylated Sn site	24
4.3	Hydride transfer for glucose isomerization in the monodentate mode with methoxylated Sn site	25
4.4	Initial proton transfer for glucose transformations in the bidentate mode with methoxylated Sn site	26
4.5	Hydride transfer for glucose transformations in the bidentate mode with methoxylated Sn site	27
4.6	Proton transfer to form complete fructose molecule in the bidentate mode with methoxylated Sn site	28

4.7	Initial proton transfer for glucose transformations in the monodentate mode with methoxylated Si site	30
4.8	Hydride transfer for glucose isomerization in the monodentate mode with methoxylated Si site	31
4.9	Initial proton transfer for glucose transformations in the bidentate mode with methoxylated Si site	32
4.10	Hydride transfer for isomerization in the bidentate mode with methoxylated Si site	33
4.11	Proton transfer to form complete fructose molecule in the bidentate mode with methoxylated Si site	34
5.1	Epimerization scheme	36
5.2	Bilik mechanism for glucose epimerization in the monodentate mode with methoxylated Sn site	38
5.3	Bilik mechanism for epimerization in the bidentate mode with methoxylated Sn site	39
5.4	Proton transfer to form complete mannose molecule in the bidentate mode with methoxylated Sn site	40
5.5	Bilik mechanism for epimerization in the monodentate mode with methoxylated Si site	42
5.6	Bilik mechanism for epimerization in the bidentate mode with methoxylated Si site	43
5.7	Proton transfer to form complete mannose molecule in the bidentate mode with methoxylated Si site	44

CHAPTER 1

INTRODUCTION

As non-renewable resources are being quickly depleted, the need to vary fuel supplies has increased. Biomass is a source of organic carbon, and in turn, provides a possibility for producing a sustainable source of energy, biofuel [26]. Data collected by the International Energy Agency (IEA) in 2012 show that 10% of the world's total primary energy supply is from biofuels and waste, and by 2030, it is predicted that 20% of transportation fuel and 25% of chemicals in the U.S. will be obtained from biomass, signifying a shift to a carbohydrate-based economy [1, 24]. The development and discovery of new technologies will facilitate the shift towards energy produced through biomass, thereby providing carbon neutral sources of energy.

Biomass is composed primarily of cellulose and hemicellulose. These two constituents make up 60-90 wt% of biomass [24]. Lignin is the primary component of the rest of biomass. Hemicellulose is a polymer of five sugars: xylose, arabinose, galactose, glucose, and mannose. The most abundant of these sugars is xylose, which is the monomer of xylan. Unlike hemicellulose, cellulose is a polymer of only one sugar, glucose. The chemical structures of xylan and cellulose are show in Figure 1.1.

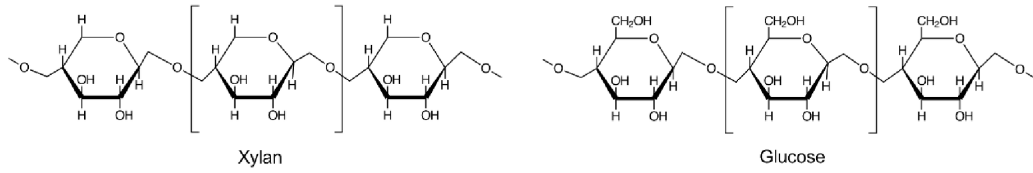


Figure 1.1

Chemical structures of xylan and cellulose

Cellulosic material can be transformed into biofuel. A simple schematic for conversion of cellulose to a biofuel is illustrated below in Figure 1.2.

As can be seen from Figure 1.2, hydrolysis of cellulose produces glucose monomers, and dehydration of glucose leads to the formation of platform chemicals, such as 2, 5-hydroxymethylfurfural (HMF). From HMF other chemicals, monomers, and in the sense of achieving a sustainable source of energy, fuels such as dimethylfuran (DMF), a liquid biofuel, can be produced. DMF can be formed through the dehydrogenation of HMF. The conversion of cellulose to a biofuel is hindered by the dehydration of glucose to a platform chemical; however, if glucose is first isomerized to fructose, with dehydration of fructose occurring after, higher yields of the platform chemical can be achieved [24].

Glucose isomerization to fructose is catalyzed in industry through the enzyme D-glucose/xylose isomerase (glucose isomerase, GI) [6]. The use of glucose isomerase is mostly in the production of high fructose corn syrup, which is used to replace the use of sucrose as a sweetener. Because of this, the enzyme has a hold over one of the largest markets in the food industry [6]. Although isomerization catalyzed with GI offers high selectivity and no side product formation, process conditions such as temperature and pH

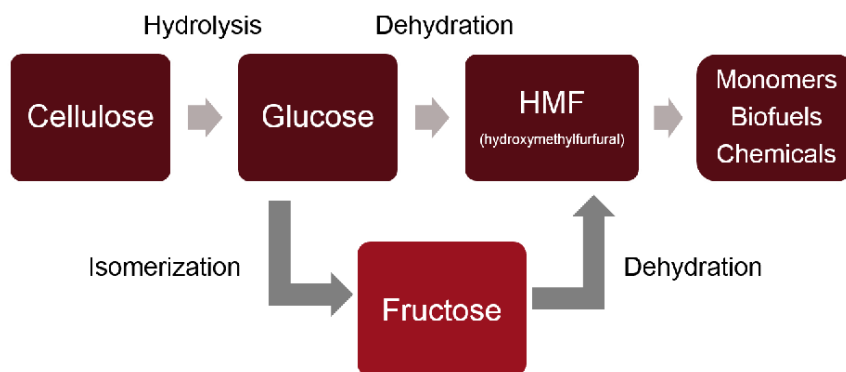


Figure 1.2

Conversion of cellulose into a platform chemical

must be regulated [6]. In addition, impurities that inhibit the enzyme must be removed from the reaction feed, and the enzyme itself must be replaced because of decrease in activity, resulting in higher operating costs [31].

Moliner et al. [31] proposed Sn-Beta zeolite as a suitable heterogeneous catalyst for glucose isomerization based on evidence provided by Corma et al. [13] that Sn-Beta proficiently catalyzes Meerwein-Ponndorf-Verley reactions (reduction of aldehydes and ketones) and Oppenauer oxidation of alcohols (together, MPVO reactions). Corma et al. [14] also showed that Sn-Beta zeolite was an efficient catalyst for Baeyer-Villiger oxidation reactions. Indeed, Moliner et al. [31] observed Sn-Beta catalyzing glucose isomerization to fructose with high selectivity and yield in aqueous reaction medium, as well as demonstrated the viability of using the zeolite in highly acidic environments and over a range of temperatures. The ability to use Sn-Beta zeolite in acidic environments opens the possibility of “one-pot” synthesis of the platform chemical HMF [33].

According to Newsam et al [32], beta zeolite is a high-silica, large pore crystalline material. Using various characterization tools—electron microscopy, electron and powder X-ray diffraction, and computer-assisted modelling—the beta framework was determined to be a three-dimensional framework, which is a hybrid of two distinct structures, consisting of twelve rings [32]. Figure 1.3 is an illustration of an extended unit cell of the beta zeolite framework, depicted molecularly. Purple and red spheres are Si and O atoms, respectively.

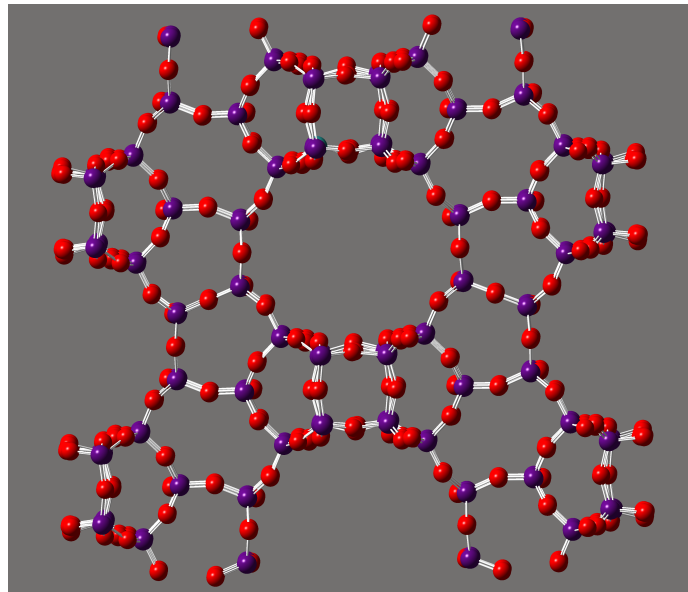


Figure 1.3

Molecular structure of beta zeolite framework

Newsam et al. [32] concluded that beta zeolite has nine distinct tetrahedral sites (T-sites), which are the positions of Si atoms that can be replaced by metal centers, such as Sn (forming Sn-Beta). The incorporation of these metal centers greatly increases the Lewis

acidity of the zeolite and allows the zeolite to coordinate and react with carbonyl groups [35]. Furthermore, beta zeolite is also a hydrophobic zeolite, allowing for a nearly water-free environment for catalysis to take place [16], and the pore size is approximately 0.8 nm, large enough for a glucose molecule to diffuse [31].

The active site for glucose transformations has been difficult to discern by past studies. Boronat et al. [7] proposed framework Sn sites has two forms: closed, a fully coordinated Sn site ($\text{Sn}-(\text{O}-\text{Si})_3$), and open, a partially hydrolyzed Sn site ($(-\text{Si}-\text{O})_3\text{SnOH}$), as shown in Figure 1.4. Because the Sn site is partially hydrolyzed, the resultant is the formation of an adjacent silanol (SiOH) group. Evidence from computational examinations of the Sn site suggests that the open Sn site is more reactive and is the active site for glucose isomerization [7, 3].

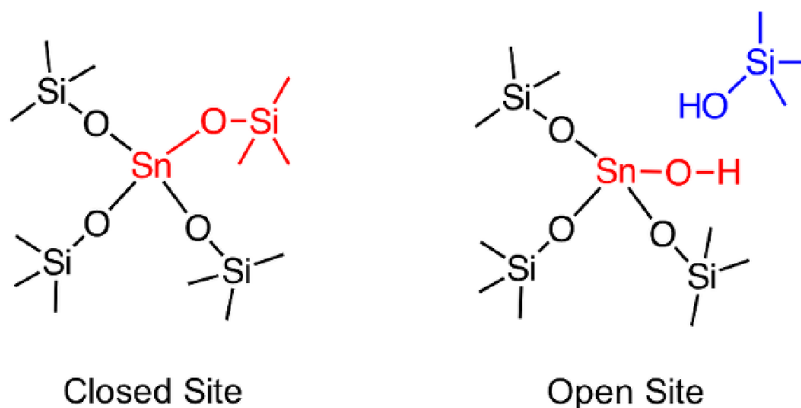


Figure 1.4

Framework Sn sites in Sn-Beta zeolite in closed and open forms

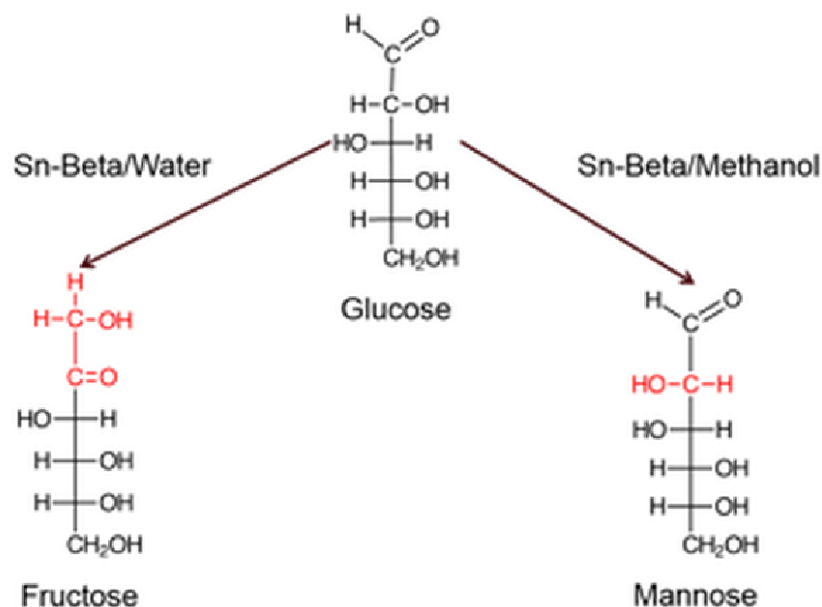


Figure 1.5

Scheme illustrating how reaction medium affects glucose transformation

Bermejo-Deval et al. [4] have shown experimentally that Sn-Beta predominantly isomerizes glucose in aqueous solution, while glucose predominantly epimerizes to mannose in methanol reaction medium. This scheme is seen in Figure 1.5. They posited that methanol could coordinate with the open Sn site, which could affect the binding of glucose to the site [4]. Several studies have provided evidence that methanol can interact with Sn sites, though the mechanistic role of the effect of methanol has not been explored or quantified [30, 38, 17].

While studies regarding glucose transformations with Sn-Beta focused on the role of the open Sn site, Rai et al. [34] employed density functional calculations to determine the role of the neighboring silanol group to the Sn site on reaction pathways. Their calculations

show that isomerization prevails when glucose binds to the Sn site that involves the silanol group, whereas epimerization prevails if glucose binds that does not include the silanol group. From their results, Rai et al. [34] speculated that in methanol medium, it was possible that silanol groups could be methoxylated, thereby promoting the binding mode that led to a pathway in which epimerization would more likely occur.

The goal of the present work is to study the effect that methanol could have on the environment of the active site of Sn-Beta. Specifically, the speculation of Rai et al. [34] is considered, and reaction pathways and energy barriers are calculated for glucose transformations when either the Sn or Si site is methoxylated. To determine these consequences, density functional theory calculations are employed.

CHAPTER 2

COMPUTATIONAL DETAILS

Density functional theory (DFT) calculations were used to determine reaction pathways and energetics. Two theorems by Hohenberg and Kohn [23] and a method approach by Kohn and Sham [27] provide the foundation for modern density functional theory.

2.1 First Hohenberg-Kohn Theorem

The first Hohenberg-Kohn theorem states that the external potential, $v(\mathbf{r})$, influencing a system of particles is uniquely (to within a constant) determined by the ground state particle density $n(\mathbf{r})$. From this theorem, it follows that any property of a system can be described in terms of the particle density $n(\mathbf{r})$ [23]. The following proof by contradiction by Hohenberg and Kohn [23] is shown for this first theorem.

The electronic density in the ground state, Ψ , is denoted as

$$n(\mathbf{r}) \equiv (\Psi, \psi^*(\mathbf{r})\psi(\mathbf{r})\Psi) \quad (2.1)$$

It can be seen that $n(\mathbf{r})$ is a functional (function of a function) of an external potential $v(\mathbf{r})$ acting on the system. It is assumed that another potential, $v'(\mathbf{r})$, with ground state, Ψ' , results in the same density $n(\mathbf{r})$. Unless $v'(\mathbf{r}) - v(\mathbf{r}) = \text{constant}$, then the two ground

states, Ψ and Ψ' , are not equal because they satisfy different Schrödinger equations. If the Hamiltonian and ground-state energies associated with Ψ are H and E , and the for Ψ' are H' and E' , then

$$E' = (\Psi', H'\Psi') < (\Psi, H'\Psi) = (\Psi, (H + V' - V)\Psi) \quad (2.2)$$

and

$$E' < E + \int [v'(\mathbf{r}) - v(\mathbf{r})]n(\mathbf{r})d\mathbf{r} \quad (2.3)$$

When the unprimed and primed quantities are exchanged,

$$E < E' + \int [v(\mathbf{r}) - v'(\mathbf{r})]n(\mathbf{r})d\mathbf{r} \quad (2.4)$$

When Equation (2.3) and Equation (2.4) are added, the following equation results, which is a contradiction.

$$E + E' < E + E' \quad (2.5)$$

2.2 Second Hohenberg-Kohn Theorem

The second theorem defines a functional for energy $E[n]$ in terms of the electronic density, which is valid for any external potential. The minimal value of the energy functional

is the ground state energy, and the corresponding density is the ground state density of the system. It follows from this theorem that if the energy functional is known, the ground state energy and particle density of the system can be determined. The following proof is given for this theorem [23].

$F[n(\mathbf{r})]$, which is a universal functional, effective for any external potential and any given number of particles, is defined as in Equation (2.6).

$$F[n(\mathbf{r})] \equiv (\Psi, (T + U)\Psi) \quad (2.6)$$

For a given $v(\mathbf{r})$, the energy functional, $E_v[n]$ is defined as

$$E_v[n] = \int v(\mathbf{r})n(\mathbf{r})d(\mathbf{r}) + F[n] \quad (2.7)$$

From here, it seen that for the correct density, $E_v[n]$ is equivalent to the ground state energy.

For a system of N particles, the energy functional of Ψ' is defined as

$$\varepsilon_v[\Psi'] \equiv (\Psi', V\Psi') + (\Psi', (T + U)\Psi') \quad (2.8)$$

If Ψ' is the electronic density in the ground state associated with a different external potential, $v(\mathbf{r})$, then by Equation (2.8) and Equation (2.6),

$$\varepsilon_v[\Psi'] = \int v(\mathbf{r})n(\mathbf{r})d(\mathbf{r}) + F[n], > \varepsilon_v[\Psi'] = \int v(\mathbf{r})n(\mathbf{r})d(\mathbf{r}) + F[n] \quad (2.9)$$

2.3 Kohn-Sham Method

Kohn and Sham [27] provided a method for utilizing the theorems by Hohenberg and Kohn [23]. From Hohenberg and Kohn [23], the ground state energy of interacting particles influenced by a potential $v(\mathbf{r})$ can be written as

$$E = \int v(\mathbf{r})n(\mathbf{r}) + \frac{1}{2} \int \int \frac{n(\mathbf{r})n(\mathbf{r}')}{|\mathbf{r} - \mathbf{r}'|} d\mathbf{r}d\mathbf{r}' + G[n] \quad (2.10)$$

where $n(\mathbf{r})$ is the density and $G[n]$ is a universal functional of the density. Kohn and Sham [27] proposed that

$$G[n] \equiv T_s[n] + E_{xc}[n] \quad (2.11)$$

where $T_s[n]$ is the kinetic energy of a system of non-interacting particles with density $n(\mathbf{r})$. They defined $E_{xc}[n]$ as the exchange and correlation energy of an interacting system with density $n(\mathbf{r})$.

If the exchange-correlation energy for the system is exact, then the solution for the system is an exact solution. Therefore, choosing an exchange-correlation functional and basis sets with high-level approximations appropriate for the system is important.

2.4 Exchange Correlation Functional

The functional used for these calculations is the hybrid functional M06-2X, which is based on meta-GGA (generalized gradient approximation) approximations. This functional was developed by Zhao and Truhlar [41, 29] and provides dependable thermochemistry and represents the van der Waals interactions present in the system.

2.5 Basis Set

Basis sets are mathematical functions that are used to describe molecular orbitals [15]. Two types of basis sets are used for these calculations: Pople [22, 21, 20] and LANZDP [37, 9].

Pople [22, 21, 20] type basis sets are split-valence basis sets; core orbitals are represented by a single basis function, but valence orbitals are split into inner and outer parts. For example, the basis set 6-31G [22] is used to describe hydrogen atoms that are added to the zeolite cluster to satisfy valency, where the zeolite cluster was cut out from the larger zeolite framework. The first number (6) denotes the amount of Gaussian orbitals that make up the core. Two numbers after the hyphen signify a split-valence double-zeta basis set, which means the valence orbitals are described by two basis functions each. For example, for these hydrogen atoms, each valence shell is described by inner and outer functions, which are sums of three and one Gaussian functions, respectively [22]. The basis set 6-31+G** [22, 21, 20] is used to describe carbon, oxygen, and the rest of the hydrogen atoms. The “+” represents diffuse functions, which allows for flexibility for weakly bound

electrons to localize from the remaining electron density. The “*” represents polarization, which adds an extra set of functions to the basis set [15].

The LANZDP basis set is used to describe Sn and Si in the system [37, 9]. Incorporated into this basis set are effective core potentials (ECPs). ECPs replace combined effects of core electrons and Coloumb potentials from the atomic core with a single pseudopotential [15].

2.6 Present Density Functional Theory Calculations

All calculations were done using the software Gaussian 09, Revision C1 [18]. The ultrafine integration grid was used in all calculations. Frequency calculations were used to verify geometry minima and transition states. Geometry minima are represented by an absence of imaginary frequencies, while transition states are characterized by a single imaginary frequency. Intrinsic reaction coordinate calculations were run to certify that the transition states connect reactants to products. Electronic energies (kcal/mol) for methoxylation of sites reaction are in reference to the sum of the hydrolyzed cluster and a methanol molecule at infinite separation. Electronic energies calculated for glucose transformations are in reference to the sum of the methoxylated cluster (either at Sn or Si site) and a cyclic glucose molecule at infinite separation.

The zeolite cluster used in these calculations are based on Rai et al. [34], who constructed the creation of their cluster model on the work of Boronat et al. [7]. This cluster is built around the T9 site in beta zeolite and is constructed to uphold the structural and chemical properties of the catalyst. To create the methoxylated cluster, a methoxy group

(-OCH₃) replaced the hydroxyl group at either the Sn or Si site, and this structure was optimized. In Figure 2.1, the first cluster (a) is the one constructed by Rai et al. [34], the second cluster (b) is the methoxylated cluster at the silanol site, and the third cluster (c) is the model that is methoxylated at the stannol site. White, red, blue, teal, and purple spheres represent hydrogen, oxygen, carbon, tin, and silicon atoms, respectively. For this optimization and for all proceeding optimizations, the hydrogens added to satisfy valence on the cluster model were kept frozen, while all other atoms were allowed to relax.

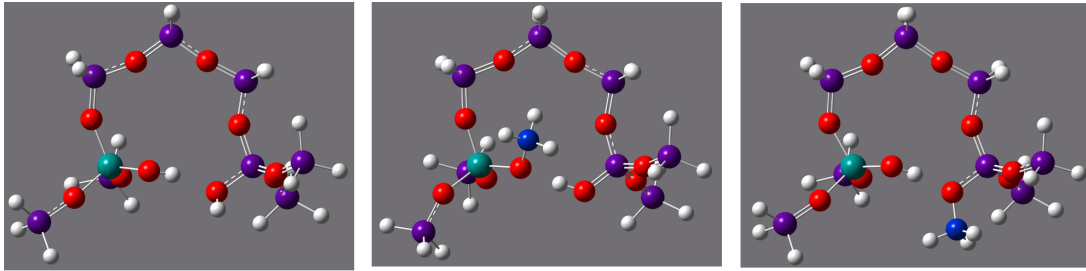


Figure 2.1

Cluster model representations of Sn-Beta zeolite

For the present study, three reactions were considered: (1) methoxylation of Sn or Si sites, (2) isomerization of glucose, and (3) epimerization of glucose. Glucose isomerization and epimerization reactions were considered with two binding modes: (1) monodentate and (2) bidentate. Rai et al. [34] defined the monodentate mode as the binding mode wherein the carbonyl group of the glucose hydrogen bonds to the silanol group. This mode allows for the silanol group to directly participate in the transition state of the reaction. The bidentate mode does not have the carbonyl group forming a hydrogen bond with the silanol group, thereby forcing silanol to remain a spectator in the reaction [34]. These schemes are illustrated in Figure 2.2. The silanol group is highlighted blue, and the carbonyl group is highlighted red. In the monodentate mode, it is seen that glucose binds so that the carbonyl group can form a hydrogen bond with the silanol group, but in the bidentate mode, the glucose molecule binds so that the silanol group does not participate in the reaction.

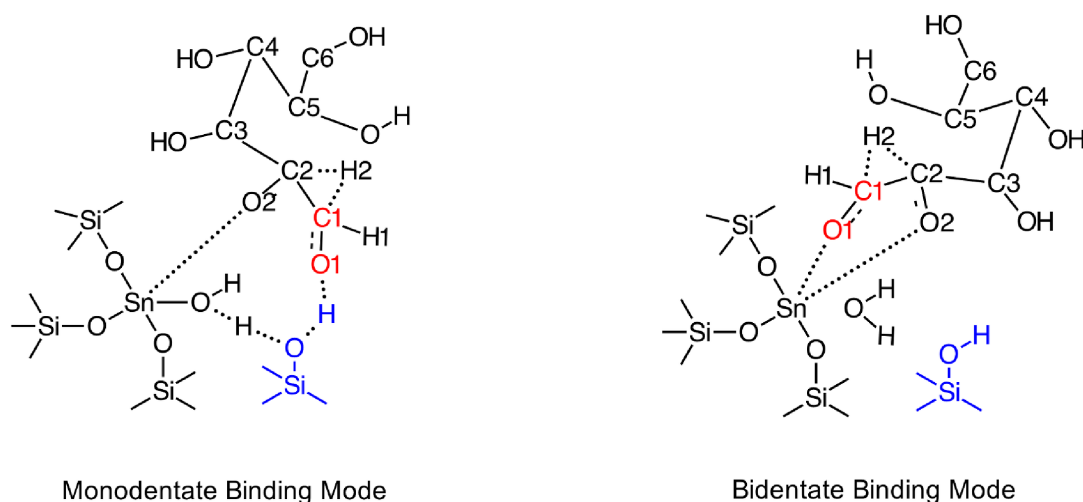


Figure 2.2

Glucose binding modes

Methoxylation of Sn or Si sites and isomerization and epimerization of glucose in the two binding modes will be discuss in the following chapters.

CHAPTER 3

METHOXYLATION OF SITES IN SN-BETA ZEOLITE

Methoxylation of sites in silicates and zeolites has been observed in previous studies [30, 17, 39, 38]. Sn and Ti atoms have larger radii in Si, so in siliceous frameworks, they can change the number of atoms they coordinate to from 4 to 5 or 6 [8]. Using diffuse reflectance ultraviolet-visible (DRUV) spectroscopy, Mal et al. [30] have observed the coordination of methanol to framework Sn sites in tin silicates. The coordination of methanol with framework Ti centers in titanium zeolites has been observed using X-ray absorption by Davis et al. [17] and in situ UV Raman studies by Wang et al. [38]. Additionally, Wang et al. [39] have observed the methoxylation of sites in zeolite when studying the conversion of methanol to dimethyl ether. These studies provide evidence that methanol can coordinate with Sn or Si sites in Sn-Beta zeolite in the form of methoxylation, but the pathway and energetics of this reaction have not been determined.

For this work, the methoxylation pathway at sites in Sn-Beta is considered to occur through a proton transfer step; methanol is deprotonated at O, and this proton forms a bond to the -OH site of the open Sn site or the silanol site. The result of this reaction is the formation of the methoxylated site and a water molecule.

3.1 Methoxylation of Sn Site

Methoxylation of the open Sn site can be seen in Figure 3.1. As can be seen in the left column (reactant of the reaction), the methanol molecule is introduced near the Sn site, and this electronic energy is calculated at -14.2 kcal/mol. In the transition state (middle column), the proton of methanol is localized between the oxygen atoms of the hydroxyl and of the methoxy group. The energy of this structure is 1.0 kcal/mol, and the activation energy is calculated at 15.2 kcal/mol. The product of methoxylation (right column) has a calculated energy of -24.6 kcal/mol.

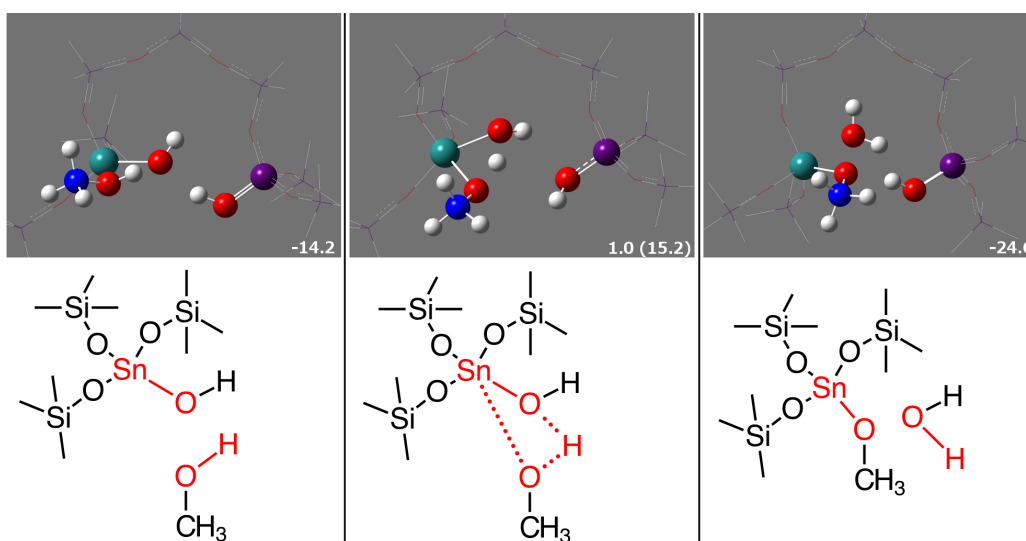


Figure 3.1

Methoxylation of Sn site in Sn-Beta zeolite

All proceeding figures regarding reaction pathways are depicted in the same way as Figure 3.1. The top row depicts atomic structures, and the bottom row illustrates the reaction mechanism scheme. Left, middle, and right columns show the reactant, transition, and product of each reaction step, respectively. Numbers denote electronic structure energies in kcal/mol, while numbers in parentheses denote activation energy.

3.2 Methoxylation of Si Site

Methoxylation of the Si site is shown in Figure 3.2. The reactant, with methanol introduced near the Si site, has a calculated electronic energy of -13.2 kcal/mol. The transition state, which has the proton of methanol localized between the -OH of silanol and the methoxy group, has an energy of 21.8 kcal/mol. The activation energy of methoxylation at the Si site is determined to be 34.9 kcal/mol. The product, which is the zeolite cluster methoxylated at the Si site and the resultant water molecule, has an energy of -12.1 kcal/mol.

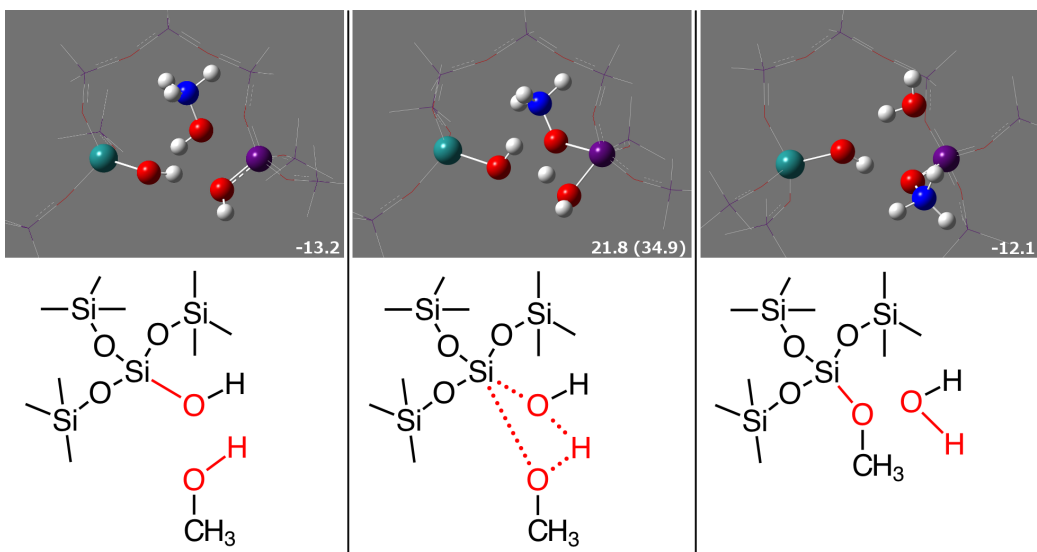


Figure 3.2

Methoxylation of Si site in Sn-Beta zeolite

3.3 Summary

As previously stated, Rai et al. [34] initially conjectured that methoxylation at the silanol site would occur in Sn-Beta zeolite, promoting glucose transformations in the bidentate mode. However, when calculating the reaction energy barrier through DFT calculations, it is determined that methoxylation at the Sn site is more favorable; the activation energy of methoxylation at the Sn site is calculated as 15.2 kcal/mol, whereas it is 34.9 kcal/mol at the Si site. In addition to the lower energy barrier for methoxylation at the Sn site, the methoxylated cluster at the Sn site is more stable by approximately 12 kcal/mol (comparison of product structures).

Although the results from these calculations are in opposition to the postulation of Rai et al. [34], these calculations suggest that methoxylation can occur at both sites, and reaction pathways are explored for both Si and Sn substituted sites to determine the effect of methoxylated sites on glucose transformations. The following sections focus on these calculations.

CHAPTER 4

GLUCOSE ISOMERIZATION WITH METHOXYLATED SITES

After glucose opens to from its cyclic structure, isomerization with Sn-Beta occurs in three steps: (1) proton transfer from the glucose molecule and binding to the active site, (2) intramolecular hydride transfer, (3) proton transfer back to sugar molecule. The resulting sugar molecule, fructose, then forms a ringed structure. This mechanism is analogous to isomerization catalyzed by metalloenzymes, as shown by Bermejo-Deval et al. [3]. The hydride transfer mechanism is an intramolecular hydrogen shift from C2 to C1 of glucose, and this mechanism has been previously studied [3, 2, 10, 11, 35, 36, 19, 12, 28].

The isomerization reaction scheme is depicted in Figure 4.1, in which X-OH is the active site of the catalyst and the Fischer projection of glucose is shown. The left column depicts the initial proton transfer. Here, the oxygen bonded to C2 (O2) is deprotonated. This proton forms a bond to the hydroxyl of the active site, while O2 forms a bond to the active site itself. The middle column shows the hydride transfer from C2 to C1 of glucose. The right column illustrates the complete fructose molecule being formed through a second proton transfer, as the proton bonded to the hydroxyl of the active site is transferred.

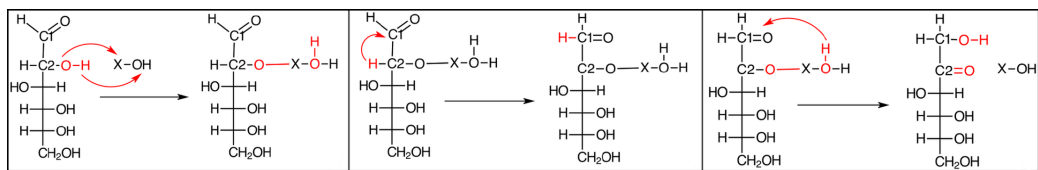


Figure 4.1

Isomerization scheme

These three steps are the focus of the current study, as glucose ring opening and ring closing of the transformed sugar molecule have been studied, and it has been shown that these are not the rate-limiting steps of the whole reaction [4, 40, 28]. As aforementioned, isomerization is considered in two binding modes: monodentate, in which the neighboring silanol group will participate in the reaction, resulting in the hydride transfer and proton transfer back to the sugar molecule to occur in one concerted step, and bidentate, in which the silanol group is a spectator and is not involved in the reaction.

4.1 Isomerization with Sn-Methoxylated Cluster

4.1.1 Monodentate Binding Mode

For the initial proton transfer, the oxygen on the C2 of glucose (O2) is deprotonated, and this proton forms a bond with the oxygen of the methoxy group. This deprotonation leads to bond formation between O2 and the active Sn site. This scheme is shown in Figure 4.2. The reactant energy, which is also considered as the initial binding energy because these calculations concern the open glucose molecule, is 6.9 kcal/mol. The transition state energy of the initial proton transfer is calculated as 15.4 kcal/mol, and it can be seen that

the proton from O2 is localized between this oxygen and the oxygen of the methoxy group. The activation energy of the initial proton transfer in the monodentate mode is calculated as 8.5 kcal/mol. The product structure is the glucose molecule, as well as methanol, being bonded to the Sn site. The calculated energy of the product structure is -2.5 kcal/mol.

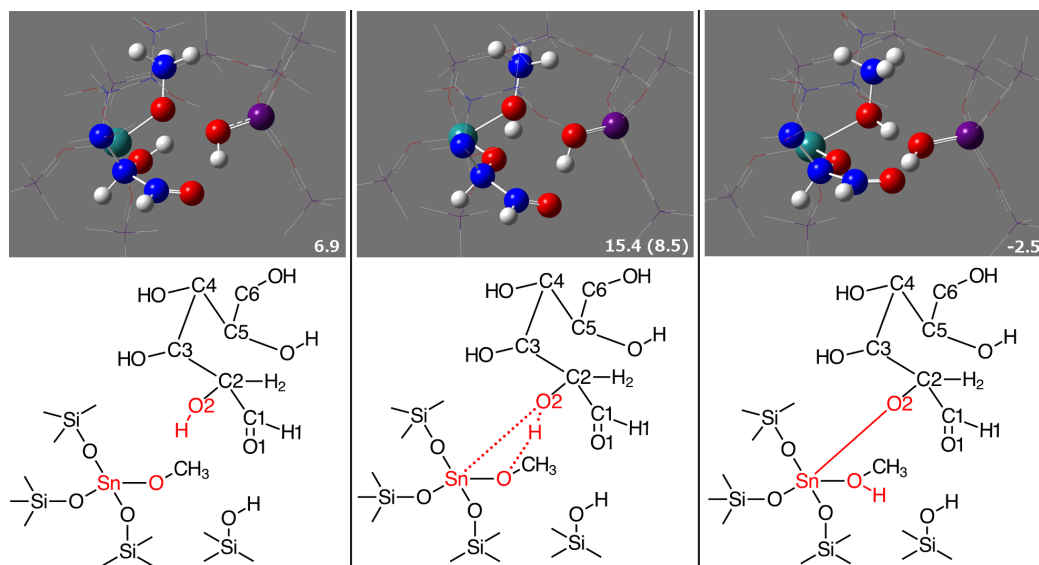


Figure 4.2

Initial proton transfer for glucose transformations in the monodentate mode with methoxylated Sn site

In the monodentate mode, the hydride shift mechanism from C2 to C1 of glucose and the proton transfer to form the complete fructose molecule occur at the same time. Therefore, in the transition state, the hydrogen on C2 shifts to C1, as the silanol and methoxy group deprotonate. The calculated energy for the transition state structure is 23.7 kcal/mol, and the activation energy for this step is 26.2 kcal/mol. The proton from the silanol group forms a bond with O1, satisfying valency and forming a complete fructose molecule, while the proton attached to the methoxy group reforms the neighboring silanol group. Figure 4.3 illustrates this step.

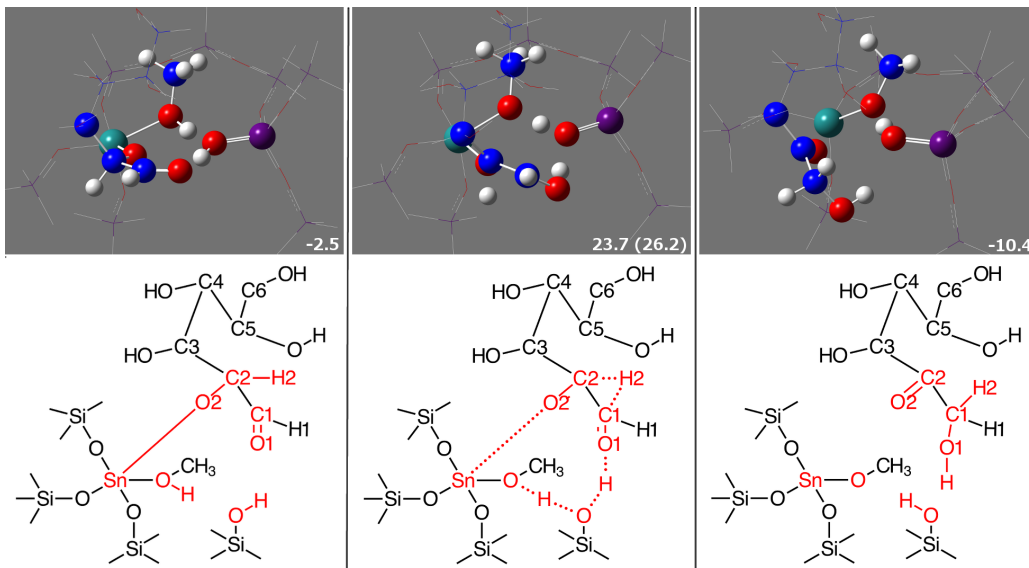


Figure 4.3

Hydride transfer for glucose isomerization in the monodentate mode with methoxylated Sn site

4.1.2 Bidentate Binding Mode

As can be seen in Figure 4.4, the initial proton transfer occurs the same way as in the monodentate mode, with deprotonation of O2 that results in glucose coordination with Sn, as well as the formation of a methanol molecule. The notable difference is that the carbonyl group (C1=O1) is situated so that it will not be able to participate in the reaction. The initial binding energy (reactant) is calculated at 4.3 kcal/mol. The transition state structure has an electronic energy of 9.6 kcal/mol. The product structure is calculated at -10.8 kcal/mol. The activation energy of the initial proton transfer step in the bidentate mode is 5.3 kcal/mol.

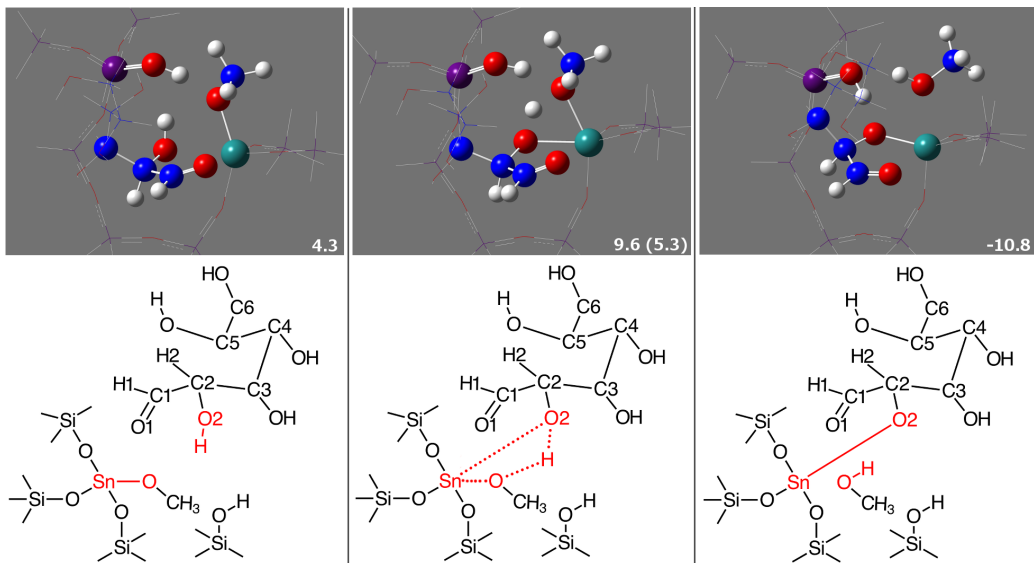


Figure 4.4

Initial proton transfer for glucose transformations in the bidentate mode with methoxylated Sn site

Because the carbonyl group cannot form a hydrogen bond with the silanol group, only the intramolecular hydride transfer from C2 to C1 occurs, which is illustrated in Figure 4.5. The transition state shows H2 shifting to C1, as well as glucose coordinating with O1 instead of O2. The activation energy for the hydride transfer is 32.7 kcal/mol. The product structure, which is O1 bonded to Sn, H2 now bonded with C1, and the carbonyl group formed with C2 and O2, has an energy of 2.9 kcal/mol.

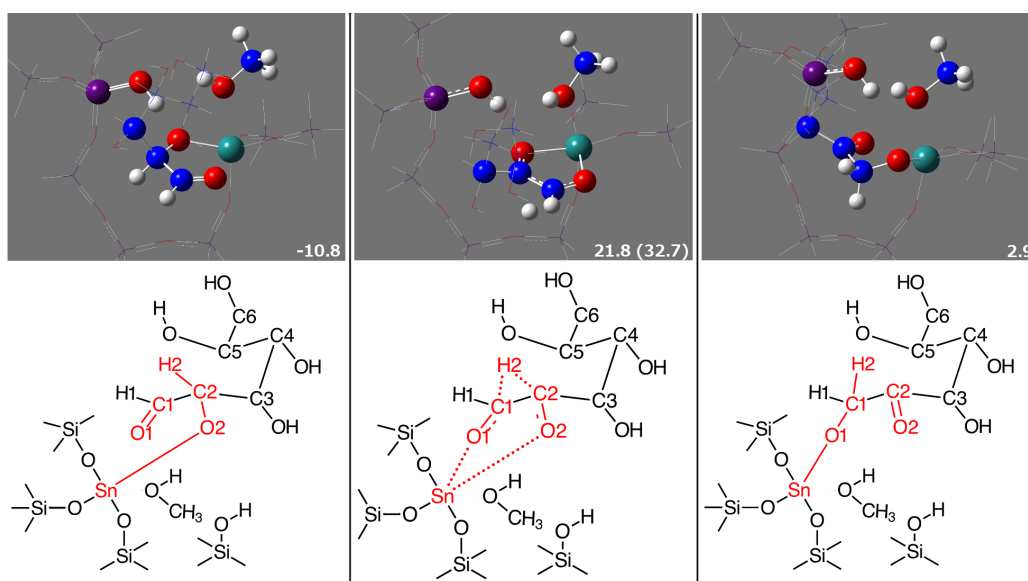


Figure 4.5

Hydride transfer for glucose transformations in the bidentate mode with methoxylated Sn site

After the hydride transfer takes place, the complete fructose molecule must be formed, and, as is illustrated in Figure 4.6, this occurs through methanol being deprotonated. In the transition state, the proton from methanol is localized between O1 and the methoxy group. The product is the reformed Sn-methoxylated zeolite and fructose sugar molecule. The product structure has an energy of -3.4 kcal/mol, and the activation energy from the proton transfer back step is calculated as 7.4 kcal/mol.

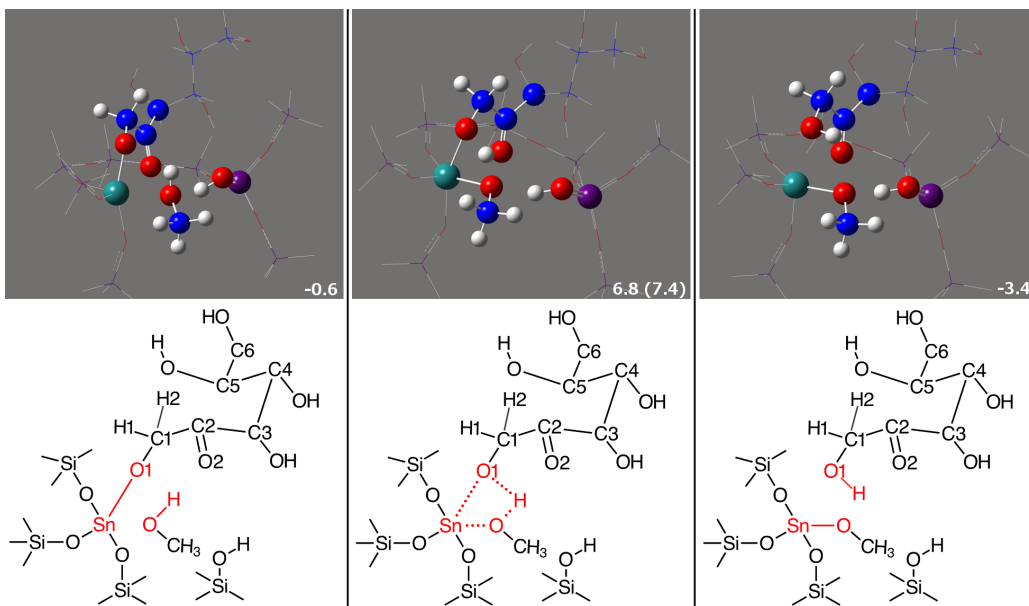


Figure 4.6

Proton transfer to form complete fructose molecule in the bidentate mode with methoxylated Sn site

4.1.3 Summary

A table summarizing activation energies for each step of isomerization in both the monodentate and bidentate mode when the Sn site is methoxylated in the Sn-Beta zeolite cluster is shown in Table 4.1.

Rai et al. [34] calculated the activation energy of hydride transfer is lower in the monodentate mode than in the bidentate mode, suggesting that the participation of the adjacent silanol group is beneficial for the isomerization reaction. The notable difference between the results obtained from Rai et al. and the present ones is the initial proton transfer energy trends. Rai et al. [34] reported that the monodentate mode had a lower activation energy, as well as a lower binding energy and more stable product structure after the initial proton transfer when stannanol and silanol groups are present. Current calculations suggest although methoxylation at the Sn site promotes the bidentate binding mode, the presence and, more importantly, the involvement of the adjacent silanol group pushes the reaction toward isomerization.

Table 4.1

Activation Energies (kcal/mol) for Glucose Isomerization with Methoxylated Sn Site

Mechanism ¹²	IPT	HT	PTB
MD	8.5	26.2	–
BD	5.3	32.7	7.4

¹MD: monodentate binding mode; BD: bidentate binding mode; IPT: initial proton transfer; HT: hydride transfer; PTB: proton transfer back.

²All proceeding tables with these abbreviations will refer to these meanings.

4.2 Isomerization with Si-Methoxylated Cluster

4.2.1 Monodentate Binding Mode

The initial proton transfer in the monodentate mode with a Si-methoxylated cluster is shown in Figure 4.7. The configuration of the reactant has an electronic energy of -12.5 kcal/mol. In the transition state structure, the proton deprotonated from O2 is localized between O2 and the hydroxyl of stannanol. The product of the initial proton transfer, which has an energy of -17.1 kcal/mol, illustrates glucose and a water molecule bonded to the Sn site. The activation energy for the initial proton transfer is calculated at 13.0 kcal/mol.

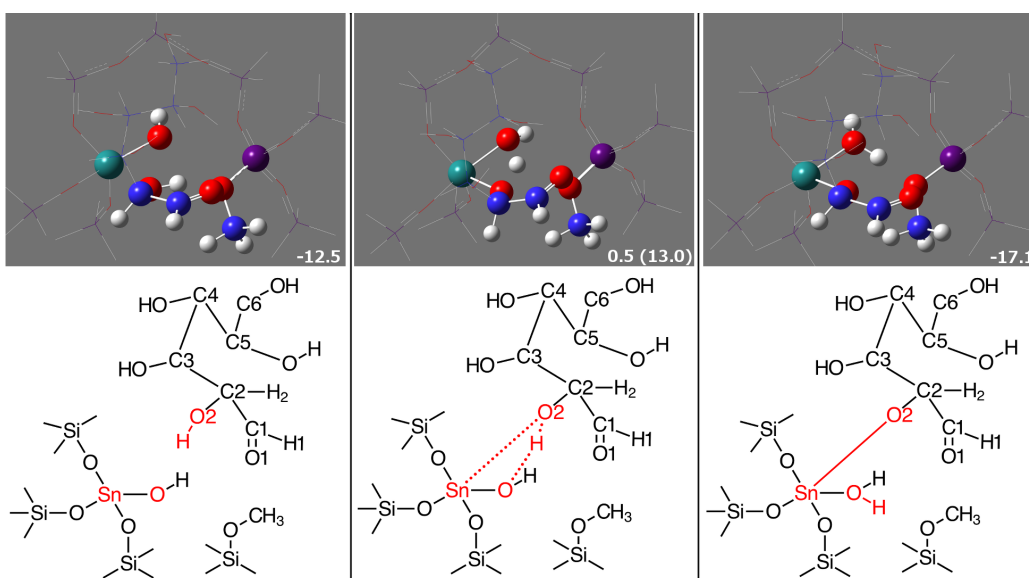


Figure 4.7

Initial proton transfer for glucose transformations in the monodentate mode with methoxylated Si site

When exploring the reaction pathway for glucose isomerization in the monodentate mode, it can be seen from Figure 4.8 that isomerization does not occur. The methoxy group attached to the silica atom does not provide the same cooperativity as the hydroxyl group, which enables the formation of a fructose molecule. Although the C2-to-C1 hydride transfer does occur, which can be seen in the product structure, there is no proton transfer from the methoxy group to O1 of the sugar molecule.

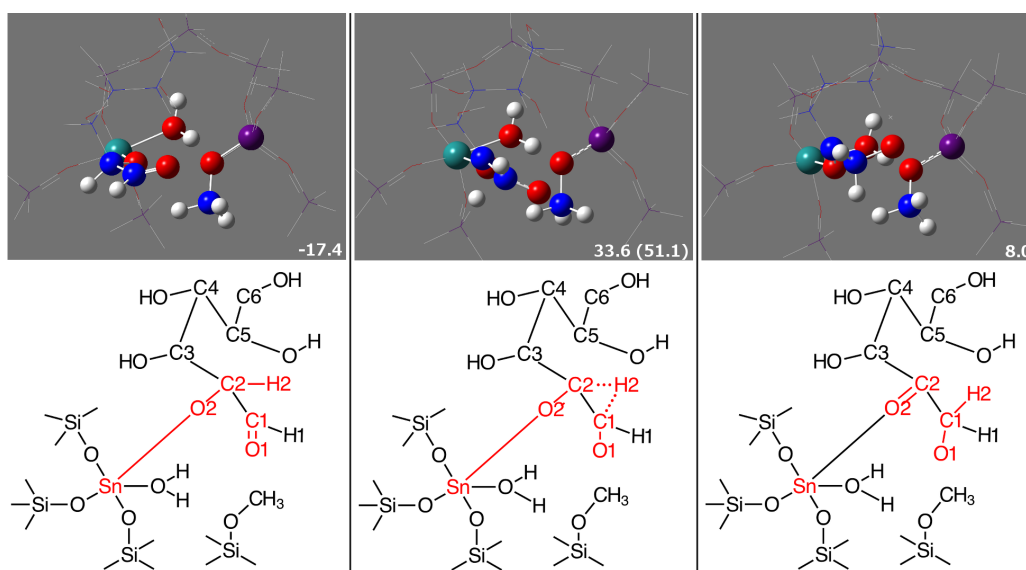


Figure 4.8

Hydride transfer for glucose isomerization in the monodentate mode with methoxylated Si site

4.2.2 Bidentate Binding Mode

The initial proton transfer in the bidentate mode when the silanol group is methoxylated is shown in Figure 4.9. The initial binding energy is calculated at -26.6 kcal/mol, and from this reactant configuration, it can be seen that glucose is introduced so that the carbonyl group will not interact with the methoxylated silanol group. The product of this proton transfer has an energy of -33.8 kcal/mol, and the energy barrier for this step is 7.0 kcal/mol.

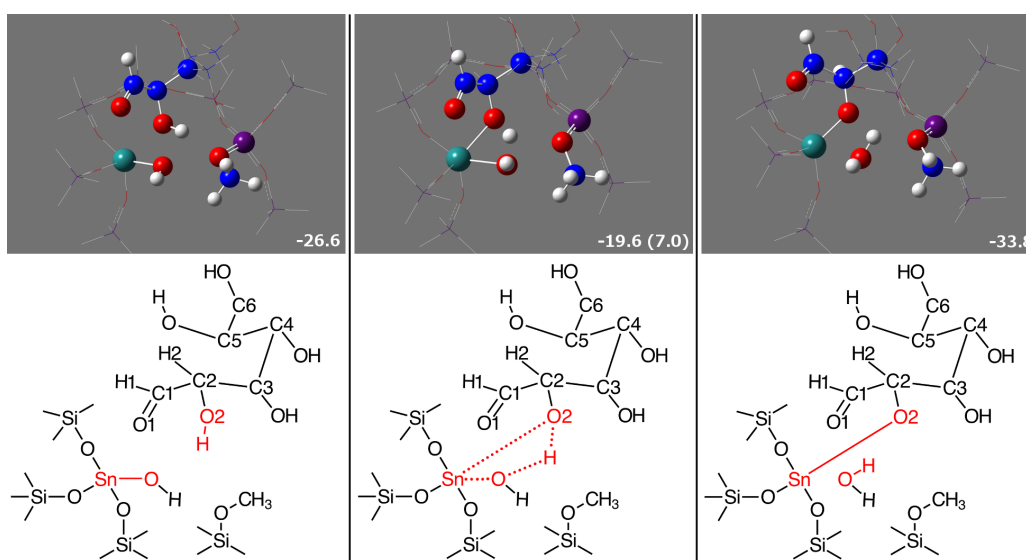


Figure 4.9

Initial proton transfer for glucose transformations in the bidentate mode with methoxylated Si site

Unlike in the monodentate mode, isomerization can occur in the bidentate mode with the Si-methoxylated cluster. Figure 4.10 depicts the intramolecular hydride transfer step, and Figure 4.11 illustrates the formation of fructose through a proton transfer. In Figure 4.10, H2 shifts to the C1 location, while the glucose molecule changes its coordination to the Sn atom from O2 to O1, as C2 and O2 become a carbonyl group. The activation energy for this step is 28.4 kcal/mol. The activation energy for the proton transfer step is calculated at 7.1 kcal/mol, and it can be seen in Figure 4.11 that a proton from the water molecule formed in the initial proton transfer step localizes between O1 and –OH. The open Sn site reforms while the glucose molecule is completely isomerized.

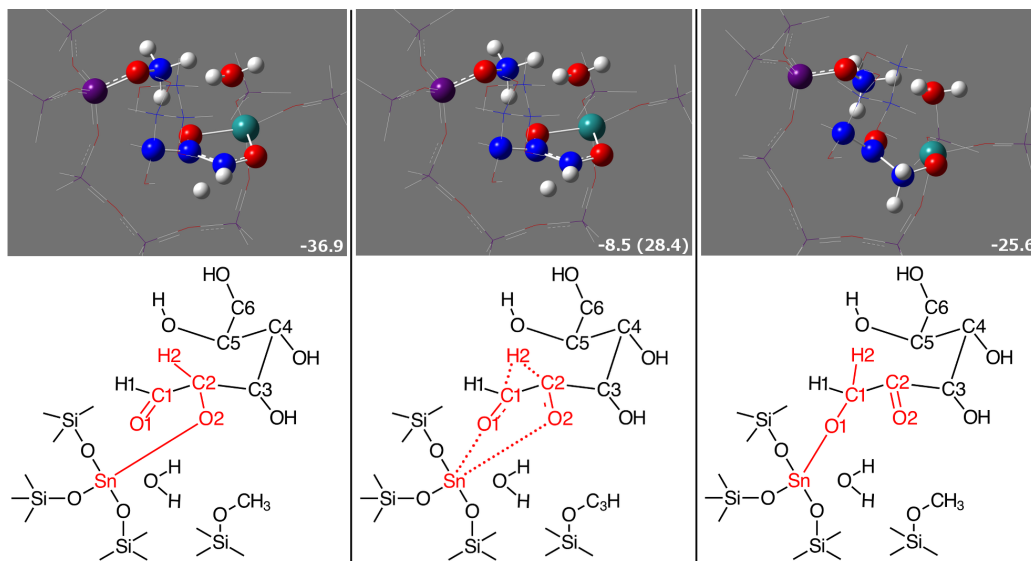


Figure 4.10

Hydride transfer for isomerization in the bidentate mode with methoxylated Si site

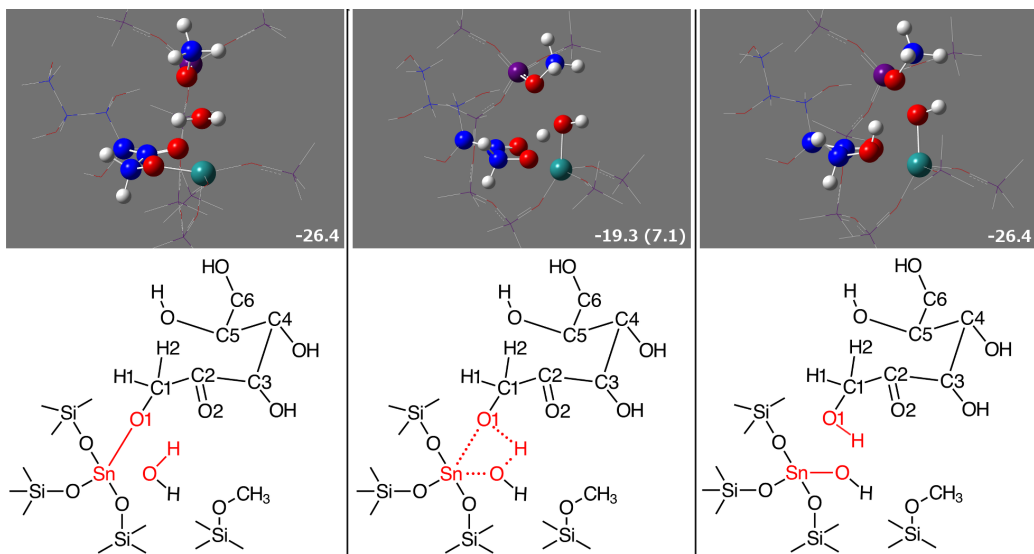


Figure 4.11

Proton transfer to form complete fructose molecule in the bidentate mode with methoxylated Si site

4.2.3 Summary

Glucose isomerization does not occur in the monodentate mode when the Si site is methoxylated. Although the intramolecular hydride transfer does take place, the methoxy group on the adjacent silanol does not provide a proton to complete the concerted proton transfer step to form the fructose molecule. In the bidentate mode, however, because the neighboring methoxylated silanol group is not involved in the reaction, a fructose molecule can form in two consequential steps: C2-to-C1 hydride transfer and a proton transfer.

CHAPTER 5

GLUCOSE EPIMERIZATION WITH METHOXYLATED SITES

As previously mentioned, the three steps focused on in this present work for isomerization catalyzed by Sn-Beta zeolite are: (1) proton transfer from the sugar molecule and binding to the active site, (2) intramolecular hydride transfer, (3) proton transfer back to sugar molecule. Epimerization occurs through a similar mechanism, except for an intramolecular hydride transfer, the Bilik mechanism occurs [4]. For the Bilik mechanism, a C2-C3 bond cleavage occurs simultaneously with C1-C3 bond formation. Figure 5.1 illustrates these three steps, where X-OH is the active site and glucose is represented in its Fischer projection.

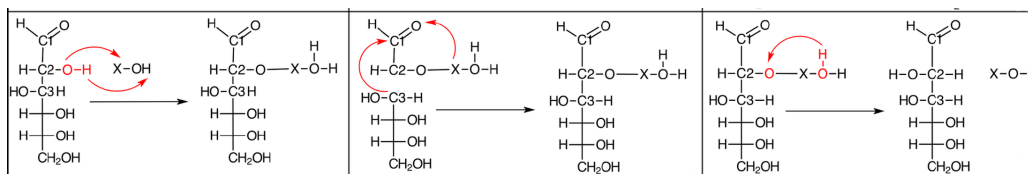


Figure 5.1

Epimerization scheme

The left column shows the initial proton transfer and glucose binding to the active site. The middle column is the Bilik mechanism, where the bond between C3 and C2 is broken, while a bond between C3 and C1 is formed. The right column illustrates the second proton transfer, where the deprotonated mannose molecule is formed.

Again, these three steps are considered with either Sn or Si sites methoxylated and in either monodentate or bidentate glucose binding modes. The initial proton transfer steps are the same for epimerization as they are for isomerization. Therefore, for the Sn-methoxylated cluster, the configurations and energetics in the monodentate mode and bidentate for the initial proton transfer is shown in Figure 4.2 and Figure 4.4, respectively; for the Si-methoxylated cluster, the configurations and energetics in the monodentate and bidentate mode for the initial proton transfer step is illustrated in Figure 4.7 and Figure 4.9, respectively. The following sections, then, will only discuss the Bilik mechanism in each mode, and additionally, the proton transfer back step in the bidentate mode.

5.1 Epimerization with Sn-Methoxylated Site

5.1.1 Monodentate Binding Mode

The reactant, transition state, and product structures of the Bilik mechanism are shown in Figure 5.2. Because glucose binds in the monodentate mode, the C3-C2 bond scission and C3-C1 bond formation and the proton transfer to form the mannose molecule occur in one combined step. The reactant, which has an energy of -2.5 kcal/mol, has the carbonyl group of glucose able to form a hydrogen bond between the adjacent silanol group. The product configuration illustrates the deprotonated form of mannose, as well as a re-

formed silanol group, which occurred through the Bilik mechanism, as well as two proton transfers—one from the $-\text{OHCH}_3$ group and one from the SiOH group. The activation energy for this step is calculated as 30.4 kcal/mol.

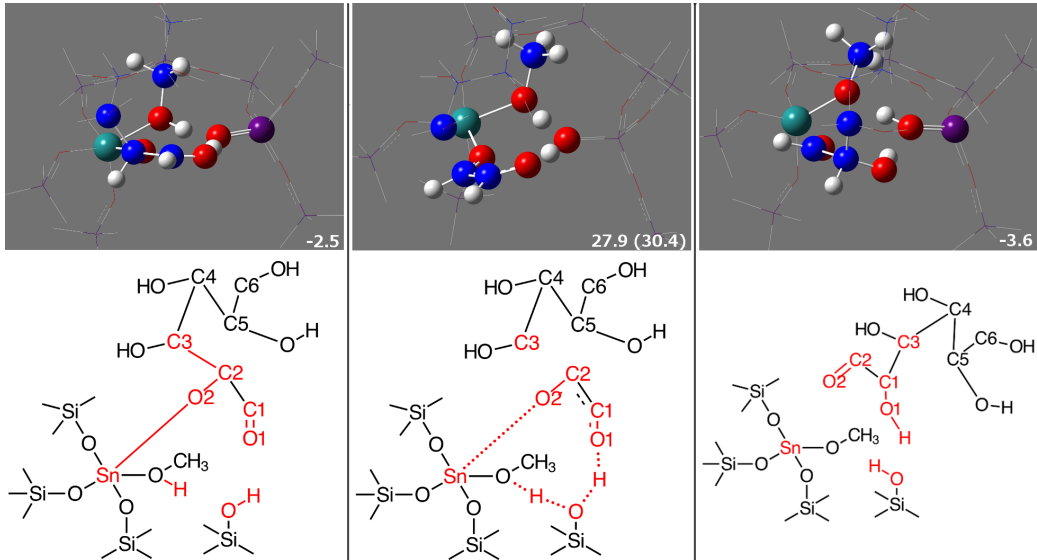


Figure 5.2

Bilik mechanism for glucose epimerization in the monodentate mode with methoxylated Sn site

5.1.2 Bidentate Binding Mode

When mannose is formed through the bidentate mode (Figure 5.3), after the first proton transfer, initially, only the bond cleavage and formation occurs. It can also be seen that the sugar molecule coordinates to Sn through O1, not O2 as is shown in the reactant configuration. The activation energy for the Bilik mechanism in the bidentate mode using the Sn-methoxylated cluster is 20.3 kcal/mol.

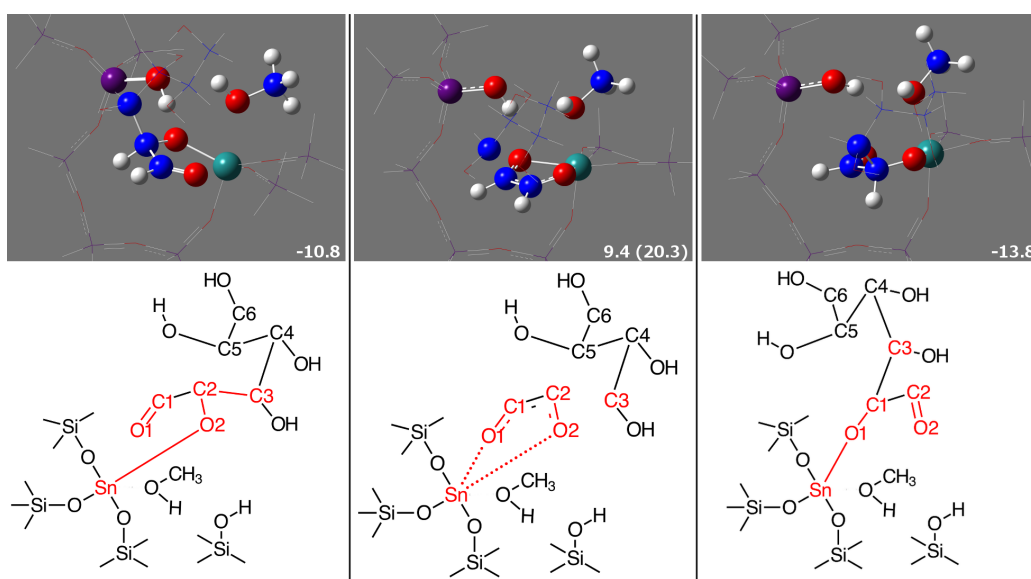


Figure 5.3

Bilik mechanism for epimerization in the bidentate mode with methoxylated Sn site

The proton transfer step for the bidentate mode is shown in Figure 5.4, occurring at a calculated activation energy of 17.6 kcal/mol. The open form of mannose is formed as the proton from methanol protonates the sugar molecule at the O1 position, reforming the methoxylated Sn site.

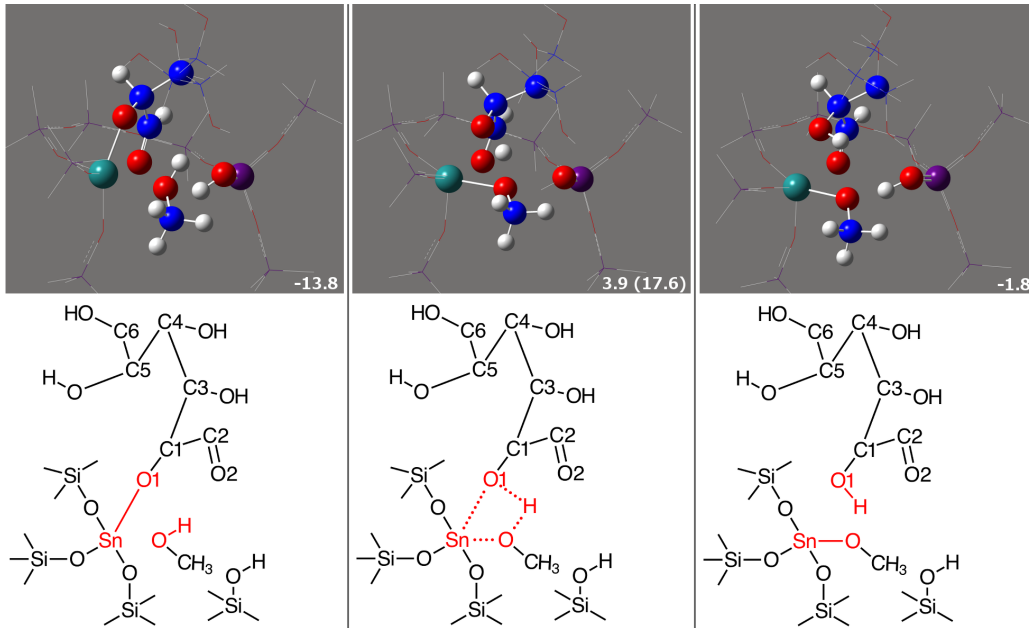


Figure 5.4

Proton transfer to form complete mannose molecule in the bidentate mode with methoxylated Sn site

5.1.3 Summary

Table 5.1

Activation Energies (kcal/mol) for Glucose Epimerization with Methoxylated Sn Site

Mechanism	IPT	Bilik	PTB
MD	8.5	30.4	–
BD	5.3	20.3	17.6

Table 5.1 records the activation energies for epimerization when the Sn site is methoxylated in each binding mode. It is concluded that epimerization is more energetically favorable in the bidentate mode, when the silanol group does not participate. This conclusion is the same as those Rai et al. [34] have reported.

5.2 Epimerization with Si-Methoxylated Site

5.2.1 Monodentate Binding Mode

As was observed with isomerization in the monodentate mode with the Si site methoxylated, epimerization, too, does not occur. In Figure 5.5, it can be seen that the bond cleavage and formation needed for the Bilik mechanism does not occur, nor does the proton transfer to form a mannose molecule.

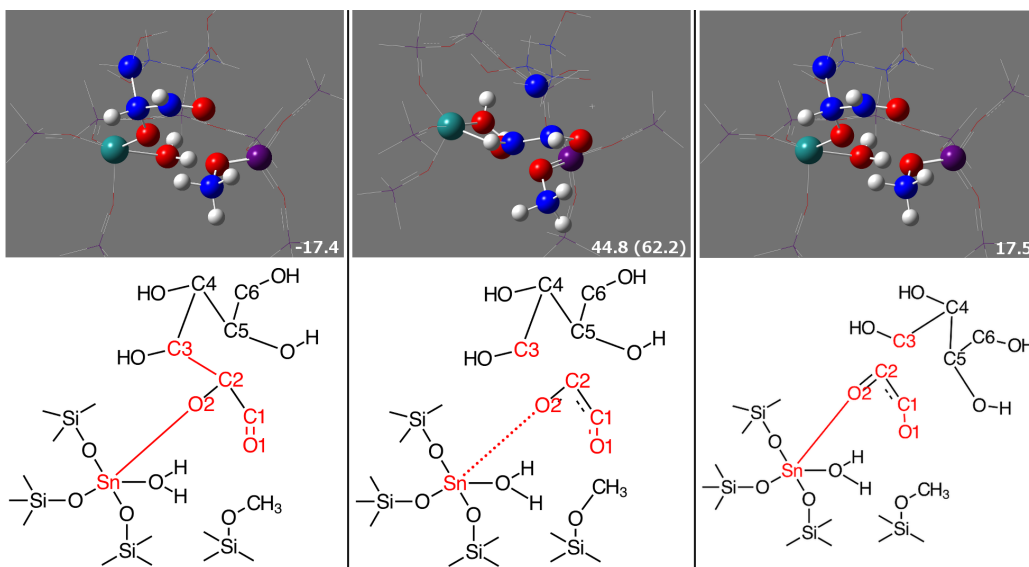


Figure 5.5

Bilik mechanism for epimerization in the monodentate mode with methoxylated Si site

5.2.2 Bidentate Binding Mode

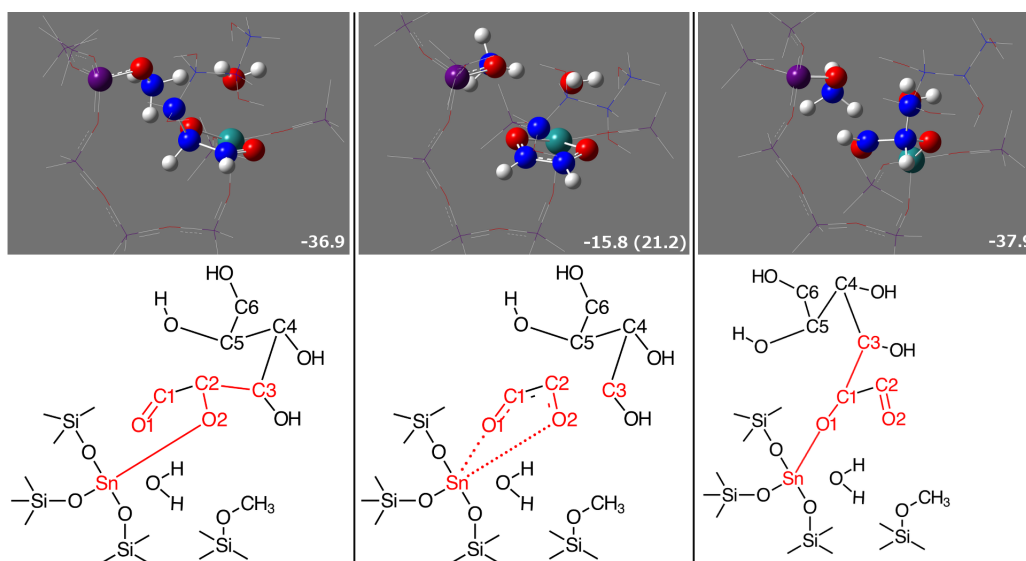


Figure 5.6

Bilik mechanism for epimerization in the bidentate mode with methoxylated Si site

The Bilik mechanism in the bidentate binding mode with a methoxylated Si site is shown in Figure 5.6. Again, because this reaction occurs in the bidentate mode, the silanol group (in this case, the methoxylated silanol group) does not participate in the reaction. The reactant configuration shows glucose bound to the Sn site, which provides stability for the Bilik mechanism to occur. The product structure shows C3-C2 scission and C3-C1 bond formation have occurred, and coordination to the Sn site has switched from O2 to O1. The energy barrier for this step is calculated as 21.2 kcal/mol.

After the C3-C2 bond cleavage and C3-C1 bond formation occur, a proton is transferred to complete the glucose transformation and restoration of the partially hydrolyzed Sn site. This step is shown in Figure 5.7. The activation energy for this step is 19.0 kcal/mol.

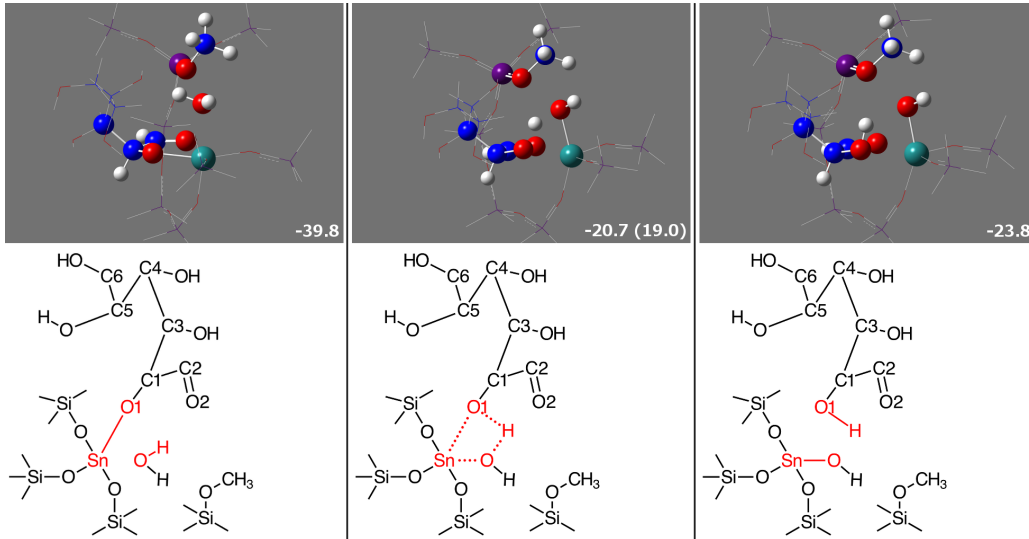


Figure 5.7

Proton transfer to form complete mannose molecule in the bidentate mode with methoxylated Si site

5.2.3 Summary

Glucose epimerization does not occur in the monodentate mode when the Si site is methoxylated. Because the Si site is methoxylated, a proton does not exist to create a hydrogen bond, which would provide valence stability and completely form the sugar molecule. When glucose binds in the bidentate mode, however, epimerization occurs through the Bilik mechanism with stability provided by the framework Sn atom.

CHAPTER 6

RESULTS AND DISCUSSION

Table 6.1 details the activation energy for the methoxylation reactions at the Sn and Si site, and it can be seen that methoxylation at the Sn Site is energetically more favorable than at the Si site. This result is in difference to what was originally speculated [34].

Table 6.1

Activation Energies (kcal/mol) for Methoxylation at Sn and Si Site

Site	Activation Energy
Sn	15.2
Si	34.9

Table 6.2 shows activation energies for each step in glucose transformations in each binding mode when the Sn site is methoxylated. Table 6.3 shows activation energies for each step in glucose transformations in each binding mode when the Si site is methoxylated.

Table 6.2

Activation Energies (kcal/mol) for Glucose Transformations with Methoxylated Sn Site

Mechanism	HT			Bílik	
	IPT	HT	PTB	Bílik	PTB
MD	8.5	26.2	–	30.4	–
BD	5.3	32.7	7.4	20.3	17.6

Table 6.3

Activation Energies (kcal/mol) for Glucose Transformations with Methoxylated Si Site

Mechanism	HT			Bílik	
	IPT	HT	PTB	Bílik	PTB
MD	13.0	51.1	–	62.2	–
BD	7.0	28.4	7.1	21.2	19.0

It can be seen from these tables that the rate-limiting step for isomerization is the hydride transfer step and for epimerization is the Bilik mechanism, which is in agreement with observations from previous studies [4, 40, 28].

Focusing on when the Sn site is methoxylated, the calculated results have a similar trend to what is reported by Rai et al. [34]. Isomerization is favorable when the neighboring silanol group participates directly in the hydride transfer; however, epimerization is favorable when the silanol group is a spectator and does not participate in the rate-limiting step.

When considering glucose transformations with a Si-methoxylated site, it is calculated that isomerization and epimerization do not occur in the monodentate mode; therefore, reactions only occur in the bidentate mode. The calculated energies for transformations in the monodentate mode shown in Table 6.3 can be disregarded because complete fructose or mannose molecules do not form. The epimerization pathway is more energetically favorable, with an energy barrier of 21.2 kcal/mol, approximately 7 kcal/mol lower than the isomerization pathway. Additionally, the activation energy of epimerization is comparable to the result reported experimentally (approximately 16.7 kcal/mol) with Sn-Beta in methanol reaction medium [4]. These findings suggest that the absence of the neighboring silanol site because of methoxylation from the presence of methanol solvent has a direct effect on the type of glucose transformation that occurs by promoting the bidentate mode, which leads to epimerization.

While this work was in progress, Bermejo-Deval et al. [5] explored glucose transformations with sodium-exchanged silanol groups to definitively determine the active site for

these transformations. Khouw and Davis [25] had used this technique of exchanging Na^+ onto silanol groups on open Ti sites in TS-1. By doing so, they concluded that open Ti sites were the active sites for alkane oxidation, observing that alkane oxidation was obstructed when silanol was exchanged [25]. Bermejo-Deval et al. [5] have shown that epimerization by the Bilik mechanism is observed when Na-exchanged Sn-Beta is used in either aqueous or methanol reaction medium. Glucose epimerization by the Bilik mechanism was not observed in methanol with Sn-Beta. Through ^{13}C -NMR experiments, it was indicated that the formation of mannose in methanol with Sn-Beta was likely via 1, 2 intramolecular hydride shift of fructose products. They concluded that the open Sn site with a neighboring silanol group is the active site for glucose isomerization, whereas the open Sn site with sodium-exchanged silanol group is the active site for glucose epimerization [5]. Furthermore, these findings indicate that the choice of solvent does not directly affect the type of glucose transformation that occurs, posing a disparity between their previous study [4, 5].

The current work comes to the same conclusions set by Bermejo-Deval et al. [5] and provides additional evidence for the active sites of glucose isomerization and epimerization by Sn-Beta zeolite. By altering the silanol site, either through sodium exchange or methoxylation, epimerization is promoted. The absence of the adjacent silanol group does not provide a proton that can transfer concertedly with the hydride transfer or Bilik mechanism, which is needed for glucose transformations to occur in the monodentate mode.

CHAPTER 7

CONCLUSIONS

In this study density functional theory calculations are employed to determine reaction pathways and energy barriers for glucose transformations with Sn-Beta zeolite when considering the effect of methanol medium through the methoxylation of either Sn or Si sites. It has been shown that methoxylation of the Sn site is more likely to occur energetically, which differs from previous speculation [34]. Nevertheless, calculations show that when the Sn site is methoxylated, results do not differ from what has been previously reported [34]; glucose isomerization is promoted when glucose binds in the monodentate mode, wherein the neighboring silanol group to the open Sn site participates in the reaction, but epimerization is promoted when glucose binds in the bidentate mode, preventing the silanol group from participating in the reaction. When the Si site is methoxylated, glucose transformations do not occur in the monodentate mode, as the methoxylation of the silanol group creates an absence of a proton that can hydrogen bond to the carbonyl group of glucose, leading to the inability for a fructose or mannose molecule to form. The bidentate mode, then, is promoted when the silanol site is methoxylated, and epimerization prevails with a lower activation energy.

The results of this study suggest that the presence and cooperativity of the adjacent silanol group to the open Sn site in Sn-Beta zeolite is necessary for glucose isomerization to occur. Alteration of the adjacent silanol group leads to glucose epimerization. These calculations provide additional evidence to bolster what is observed in experiment for the active sites of glucose isomerization and glucose epimerization [5]. These insights on the active sites of Sn-Beta zeolite on glucose transformations are useful for future catalyst development and design.

REFERENCES

- [1] “Key World Energy Statistics (2014),” Accessed electronically, 2014, <http://www.iea.org/publications/freepublications/publication/KeyWorld2014.pdf>.
- [2] R. S. Assary and L. A. Curtiss, “Theoretical Study of 1,2-Hydride Shift Associated with the Isomerization of Glyceraldehyde to Dihydroxy Acetone by Lewis Acid Active Site Models,” *The Journal of Physical Chemistry A*, vol. 115, 2011, pp. 8754–8760.
- [3] R. Bermejo-Deval, R. S. Assary, E. Nikolla, M. Moliner, Y. Román-Leshkov, S.-J. Hwang, A. Palsdottir, D. Silverman, R. F. Lobo, L. A. Curtiss, and M. E. Davis, “Metalloenzyme-like Catalyzed Isomerizations of Sugars by Lewis Acid Zeolites,” *Proceedings of the National Academy of Sciences of the United States of America*, vol. 109, 2012, pp. 9727–32.
- [4] R. Bermejo-Deval, R. Gounder, and M. E. Davis, “Framework and Extraframework Tin Sites in Zeolite Beta React Glucose Differently,” *ACS Catalysis*, vol. 2, 2012, pp. 2705–2713.
- [5] R. Bermejo-Deval, M. Orazov, R. Gounder, S. J. Hwang, and M. E. Davis, “Active Sites in Sn-Beta for Glucose Isomerization to Fructose and Epimerization to Mannose,” *ACS Catalysis*, vol. 4, 2014, pp. 2288–2297.
- [6] S. H. Bhosale, M. B. Rao, and V. V. Deshpande, “Molecular Industrial Aspects of Glucose Isomerase,” *Microbiological Reviews*, vol. 30, 1996, pp. 280–300.
- [7] M. Boronat, P. Concepcion, a. Corma, M. Renz, and S. Valencia, “Determination of the Catalytically Active Oxidation of Lewis Acid Sites in Sn-Beta zeolites, and Their Optimisation by the Combination of Theoretical and Experimental Studies,” *Journal of Catalysis*, vol. 234, 2005, pp. 111–118.
- [8] M. Cambor, A. Corma, and J. Perez-Pariente, “Synthesis of Titanaluminosilicates Isomorphous to Zeolite Beta, Active as Oxidation Catalysts,” *Zeolites*, vol. 13, 1993, pp. 82–87.
- [9] C. E. Check, T. O. Faust, J. M. Bailey, B. J. Wright, T. M. Gilbert, and L. S. Sunderlin, “Addition of Polarization and Diffuse Functions to the LANL2DZ Basis Set for P-Block Elements,” *The Journal of Physical Chemistry A*, vol. 105, 2001, pp. 8111–8116.

- [10] V. Choudhary, S. Caratzoulas, and D. G. Vlachos, “Insights into the Isomerization of Xylose to Xylulose and Lyxose by a Lewis Acid Catalyst,” *Carbohydrate Research*, vol. 368, 2013, pp. 89–95.
- [11] V. Choudhary, A. Pinar, R. F. Lobo, D. G. Vlachos, and S. Sandler, “Comparison of Homogeneous and Heterogeneous Catalyst for Glucose to Fructose Isomerization in Aqueous Media,” *ChemSusChem*, vol. 6, 2013, pp. 2369–2376.
- [12] V. Choudhary, A. B. Pinar, S. I. Sandler, D. G. Vlachos, and R. F. Lobo, “Xylose Isomerization to Xylulose and Its Dehydration to Furfural in Aqueous Media,” *ACS Catalysis*, vol. 1, 2011, pp. 1724–1728.
- [13] A. Corma, M. E. Domine, L. Nemeth, and S. Valencia, “Al-free Sn-Beta Zeolite as a Catalyst for the Selective Reduction of Carbonyl Compounds (Meerwein-Ponndorf-Verley Reaction),” *Journal of the American Chemical Society*, vol. 124, 2002, pp. 423–425.
- [14] A. Corma, L. T. Nemeth, M. Renz, and S. Valencia, “Sn-Zeolite Beta as a Heterogeneous Chemoselective Catalyst for Baeyer-Villiger oxidations,” *Nature*, vol. 412, 1995, pp. 423–425.
- [15] C. Cramer, *Essentials of Computational Chemistry*, second edition, John Wiley & Sons Ltd., 2004.
- [16] C. X. a. da Silva, V. L. C. Gonçalves, and C. J. a. Mota, “Water-Tolerant Zeolite Catalyst for the Acetalisation of Glycerol,” *Green Chemistry*, vol. 11, 2009, p. 38.
- [17] Z. T. J. E. W. W. S. Davis, R. J.; Liu, “X-ray absorption spectroscopy of Ti-containing molecular sieves ETS-10, aluminum-free Ti-Óé, and TS-1,” *Catalysis Letters*, vol. 34, no. 1-2, 1995, pp. 101–113.
- [18] M. J. Frisch, G. W. Trucks, H. B. Schlegel, G. E. Scuseria, M. A. Robb, J. R. Cheeseman, G. Scalmani, V. Barone, B. Mennucci, G. A. Petersson, H. Nakatsuji, M. Caricato, X. Li, H. P. Hratchian, A. F. Izmaylov, J. Bloino, G. Zheng, J. L. Sonnenberg, M. Hada, M. Ehara, K. Toyota, R. Fukuda, J. Hasegawa, M. Ishida, T. Nakajima, Y. Honda, O. Kitao, H. Nakai, T. Vreven, J. A. Montgomery, J. E. Peralta, F. Ogliaro, M. Bearpark, J. J. Heyd, E. Brothers, K. N. Kudin, V. N. Staroverov, R. Kobayashi, J. Normand, K. Raghavachari, A. Rendell, J. C. Burant, S. S. Iyengar, J. Tomasi, M. Cossi, N. Rega, J. M. Millam, M. Klene, J. E. Knox, J. B. Cross, V. Bakken, C. Adamo, J. Jaramillo, R. Gomperts, R. E. Stratmann, O. Yazyev, A. J. Austin, R. Cammi, C. Pomelli, J. W. Ochterski, R. L. Martin, K. Morokuma, V. G. Zakrzewski, G. A. Voth, P. Salvador, J. J. Dannenberg, S. Dapprich, A. D. Daniels, O. Farkas, J. B. Foresman, J. V. Ortiz, J. Cioslowski, and D. J. Fox, “Gaussian 09 Revision C.1. Gaussian,” 2009, Gaussian Inc.: Wallingford, CT.

- [19] R. Gounder and M. E. Davis, "Titanium-beta Zeolites Catalyze the Stereospecific Isomerization of D -glucose to L-sorbose via Intramolecular C5-C1 Hydride Shift," *ACS Catalysis*, vol. 3, 2013, pp. 1469–1476.
- [20] T. H. Clark, J. Chandrasekhar, G. W. Spitznagel, and P. V. R. Schleyer, "Efficient Diffuse Function-Augmented Basis Sets for Anion Calculations. III. The 3-21+G Basis Set for First-Row Elements, Li-F," *Journal of Computational Chemistry*, vol. 4, 1983, pp. 294–301.
- [21] P. Hariharan and J. Pople, "The Influence of Polarization Functions on Molecular Orbital Hydrogenation Energies," *Theoretica chimica acta*, vol. 28, 1973, pp. 213–222.
- [22] R. P. J. Hehre, W. J.; Ditchfield, "Self-Consistent Molecular Orbital Methods. XII. Further Extensions of Gaussian-Type Basis Sets for Use in Molecular Orbital Studies of Organic Molecules," *Journal of Physical Chemistry*, vol. 56, 1972, pp. 2257–2261.
- [23] P. Hohenberg and W. Kohn, "Inhomogeneous Electron Gas," *Physical Review*, vol. 136, 1964, pp. 864–871.
- [24] G. W. Huber, S. Iborra, and A. Corma, "Synthesis of Transportation Fuels from Biomass: Chemistry, Catalysts, and Engineering," *Chemical Reviews*, vol. 106, 2006, pp. 4044–4098.
- [25] C. Khouw and M. E. Davis, "Catalytic Activity of Titanium Silicates Synthesized in the Presence of Alkali-Metal and Alkaline-Earth Ions," *Journal of Catalysis*, vol. 151, 1995, pp. 77–86.
- [26] D. L. Klass, *Encyclopedia of Energy*, chapter Biomass for Renewable Energy, Fuels, and Chemicals, Elsevier.
- [27] W. Kohn and L. J. Sham, "Self-Consistent Equations Including Exchange and Correlation Effects," *Physical Review*, vol. 136, 1965, pp. 1133–1138.
- [28] Y.-P. Li, M. Head-Gordon, and A. T. Bell, "Analysis of the Reaction Mechanism and Catalytic Activity of Metal-Substituted Beta Zeolite for the Isomerization of Glucose to Fructose," *ACS Catalysis*, vol. 4, 2014, pp. 1537–1545.
- [29] M. Linder and T. Brinck, "On the Method-Dependence of Transition State Asynchronicity in Diels-Alder Reactions," *Physical chemistry chemical physics : PCCP*, vol. 15, 2013, pp. 5108–5114.
- [30] N. K. Mal and A. V. Ramaswamy, "Hydroxylation of Phenol over Sn-silicalite-1 Molecular Sieve: Solvent Effects," *Journal of Molecular Catalysis A: Chemical*, vol. 105, 1996, pp. 149–158.

- [31] M. Moliner, Y. Román-Leshkov, and M. E. Davis, “Tin-containing Zeolites are Highly Active Catalysts for the Isomerization of Glucose in Water,” *Proceedings of the National Academy of Sciences of the United States of America*, vol. 107, 2010, pp. 6164–6168.
- [32] J. Newsam, M. Treacy, W. Koetsier, and C. De Gruyter, “Structural Characterization of Zeolite Eeta,” *Proc. R. Soc. Lond. A*, vol. 420, 1988, pp. 375–405.
- [33] E. Nikolla, Y. Román-Leshkov, M. Moliner, and M. E. Davis, ““One-pot” Synthesis of 5-(hydroxymethyl)furfural from Carbohydrates Using Tin-beta Zeolite,” *ACS Catalysis*, vol. 1, 2011, pp. 408–410.
- [34] N. Rai, S. Caratzoulas, and D. G. Vlachos, “Role of Silanol Group in Sn-Beta Zeolite for Glucose Isomerization and Epimerization Reactions,” *ACS Catalysis*, vol. 3, 2013, pp. 2294–2298.
- [35] Y. Román-Leshkov and M. E. Davis, “Activation of Carbonyl-Containing Molecules with Solid Lewis Acids in Aqueous Media,” *ACS Catalysis*, vol. 1, 2011, pp. 1566–1580.
- [36] Y. Román-Leshkov, M. Moliner, J. a. Labinger, and M. E. Davis, “Mechanism of Glucose Isomerization Using a Solid Lewis Acid Catalyst in Water,” *Angewandte Chemie*, vol. 49, 2010, pp. 8954–8957.
- [37] W. R. Wadt and P. J. Hay, “Ab Initio Effective Core Potentials for Molecular Calculations. Potentials for Main Group Elements Na to Bi,” *The Journal of Chemical Physics*, vol. 82, 1985, pp. 284–298.
- [38] L. Wang, G. Xiong, J. Su, P. Li, and H. Guo, “In situ UV Raman Spectroscopic Study on the Reaction Intermediates for Propylene Epoxidation on TS-1,” *Journal of Physical Chemistry C*, vol. 105, 2012, pp. 12553–12558.
- [39] W. Wang, M. Seiler, and M. Hunger, “Role of Surface Methoxy Species in the Conversion of Methanol to Dimethyl Ether on Acidic Zeolites Investigated by in Situ Stopped-Flow MAS NMR Spectroscopy,” *The Journal of Physical Chemistry B*, vol. 105, 2001, pp. 12553–12558.
- [40] G. Yang, E. A. Pidko, and E. J. M. Hensen, “The Mechanism of Glucose Isomerization to Fructose over Sn-BEA Zeolite: A Periodic Density Functional Theory Study,” *ChemSusChem*, vol. 6, 2013, pp. 1688–1696.
- [41] Y. Zhao and D. G. Truhlar, “The M06 Suite of Density Functionals for Main Group Thermochemistry, Thermochemical Kinetics, Noncovalent Interactions, Excited States, and Transition Elements: Two New Functionals and Systematic Testing of Four M06-class Functionals and 12 Other Functionals,” *Theoretical Chemistry Accounts*, vol. 120, 2008, pp. 215–241.